frontiers in Plant Science

PERSPECTIVE
published: 15 September 2020
doi: 10.3389/fpls.2020.581851

Modeling Light Response of Electron Transport Rate and Its Allocation for Ribulose Biphosphate Carboxylation and Oxygenation

Zi-Piao Ye[1†], *Hua-Jing Kang*[2†], *Ting An*[1], *Hong-Lang Duan*[3], *Fu-Biao Wang*[1], *Xiao-Long Yang*[1*] and *Shuang-Xi Zhou*[4*]

[1] Maths and Physics College, Jinggangshan University, Ji'an, China, [2] Department of Landscape and Water Conservancy Engineering, Wenzhou Vocational College of Science and Technology, Wenzhou, China, [3] Jiangxi Provincial Key Laboratory for Restoration of Degraded Ecosystems & Watershed Ecohydrology, Nanchang Institute of Technology, Nanchang, China, [4] The New Zealand Institute for Plant and Food Research Limited, Hawke's Bay, New Zealand

OPEN ACCESS

Edited by:
Stefano Santabarbara,
National Research Council (CNR), Italy

Reviewed by:
Yanbo Hu,
Northeast Forestry University, China
John A. Morgan,
Purdue University, United States

***Correspondence:**
Shuang-Xi Zhou
shuangxi.zhou@plantandfood.co.nz
Xiao-Long Yang
yxl327813040@163.com

†These authors have contributed equally to this work

Specialty section:
This article was submitted to Plant Abiotic Stress, a section of the journal Frontiers in Plant Science

Received: 10 July 2020
Accepted: 25 August 2020
Published: 15 September 2020

Citation:
Ye Z-P, Kang H-J, An T, Duan H-L, Wang F-B, Yang X-L and Zhou S-X (2020) Modeling Light Response of Electron Transport Rate and Its Allocation for Ribulose Biphosphate Carboxylation and Oxygenation. Front. Plant Sci. 11:581851. doi: 10.3389/fpls.2020.581851

Accurately describing the light response curve of electron transport rate (J–I curve) and allocation of electron flow for ribulose biphosphate (RuBP) carboxylation (J_C–I curve) and that for oxygenation (J_O–I curve) is fundamental for modeling of light relations of electron flow at the whole-plant and ecosystem scales. The non-rectangular hyperbolic model (hereafter, NH model) has been widely used to characterize light response of net photosynthesis rate (A_n; A_n–I curve) and J–I curve. However, NH model has been reported to overestimate the maximum A_n (A_{nmax}) and the maximum J (J_{max}), largely due to its asymptotic function. Meanwhile, few efforts have been delivered for describing J_C–I and J_O–I curves. The long-standing challenge on describing A_n–I and J–I curves have been resolved by a recently developed A_n–I and J–I models (hereafter, Ye model), which adopt a nonasymptotic function. To test whether Ye model can resolve the challenge of NH model in reproducing J–I, J_C–I and J_O–I curves over light-limited, light-saturated, and photoinhibitory I levels, we compared the performances of Ye model and NH model against measurements on two C_3 crops (*Triticum aestivum* L. and *Glycine max* L.) grown in field. The results showed that NH model significantly overestimated the A_{nmax} and J_{max} for both species, which can be accurately obtained by Ye model. Furthermore, NH model significantly overestimated the maximum electron flow for carboxylation ($J_{C\text{-}max}$) but not the maximum electron flow for oxygenation ($J_{O\text{-}max}$) for both species, disclosing the reason underlying the long-standing problem of NH model—overestimation of J_{max} and A_{nmax}.

Keywords: photosynthesis, light response curve, electron flow partitioning, maximum *J*, saturation light intensity, ribulose biphosphate carboxylation, ribulose biphosphate oxygenation, model

INTRODUCTION

Light intensity (I) is one of the most important environmental drivers affecting electron flow and its allocation for carboxylation versus oxygenation of ribulose biphosphate (RuBP). At I levels before reaching saturation intensity, the non-rectangular hyperbolic model (hereafter, NH model) is a sub-model which is widely used to characterize the light-response curve of electron transport rate (J–I curve) and to estimate the maximum J ($J_{\max}$) in C_3 photosynthesis model (e.g., Farquhar et al., 1980; Farquhar and Wong, 1984; von Caemmerer, 2000; Farquhar et al., 2001; Long and Bernacchi, 2003; von Caemmerer et al., 2009; Bernacchi et al., 2013; Bellasio et al., 2015; Busch and Sage, 2017; Walker et al., 2017; Cai et al., 2018) and in C_4 photosynthesis model (Berry and Farquhar, 1978; von Caemmerer and Furbank, 1999; von Caemmerer, 2013). At light saturation, $J_{\max}$ is estimated by the C_3 photosynthesis model (Farquhar et al., 1980; von Caemmerer, 2013; Farquhar and Busch, 2017). Accurate estimation of $J_{\max}$ is important for understanding photosynthesis of C_3 and C_4 species. $J_{\max}$ is a key quantity to represent plant photosynthetic status under different environmental conditions when the net photosynthesis rate (A_n) is limited by the regeneration of RuBP, associated with the partitioning of electron flow through photosystem II (PSII) for RuBP carboxylation (J_C) versus that for RuBP oxygenation (J_O) (Farquhar et al., 1980; Long and Bernacchi, 2003).

By simulating light-response curves of photosynthesis (A_n–I curve), NH model has been widely used to obtain key photosynthetic characteristics (e.g., the maximum net photosynthetic rate, A_{nmax}; light compensation point when $A_n = 0$, I_c; dark respiration rate, R_d) for various species under different environmental conditions (e.g., Ögren & Evans, 1993; Thornley, 1998; Ye, 2007; Aspinwall et al., 2011; dos Santos et al., 2013; Mayoral et al., 2015; Sun et al., 2015; Park et al., 2016; Quiroz et al., 2017; Yao et al., 2017; Xu et al., 2019; Yang et al., 2020; Ye et al., 2020). Significant difference between observed A_{nmax} values and that estimated by NH model for various species has been widely reported (e.g., Chen et al., 2011; dos Santos et al., 2013; Lobo et al., 2014; Ogawa, 2015; Sun et al., 2015; Quiroz et al., 2017; Poirier-Pocovi et al., 2018; Ye et al., 2020). This long-standing challenge has been resolved by an A_n–I model, which adopts a nonasymptotic function and can accurately reproduce A_n–I curve over light-limited, light-saturated and photoinhibitory I levels (Ye et al., 2013) (hereafter, Ye model).

Recently, Buckley and Diaz-Espejo (2015) proposed that NH model would overestimate $J_{\max}$ due to its asymptotic function. A robust model which can accurately reproduce the observed J–I curve, and obtain $J_{\max}$, is urgently needed (Buckley and Diaz-Espejo, 2015). Furthermore, the light response of J partitioning for RuBP carboxylation and oxygenation (J_C–I and J_O–I curves), and the key quantities to describe the curves (e.g., the maximum J_C, $J_{\text{C-max}}$, and the maximum J_O, $J_{\text{O-max}}$, as well as their corresponding saturation light intensities) are rarely studied. Meanwhile, for the first time, we compared the performances of the two models in reproducing J_C–I and J_O–I curves.

This study aimed to fill these important gaps using an observation-modeling intercomparison approach. We firstly measured leaf gas exchange and chlorophyll fluorescence over a wide range of I levels for two C_3 species [winter wheat (*Triticum aestivum* L.) and soybean (*Glycine max* L.)]. We then incorporated Ye model to reproduce A_n–I, J–I, J_C–I, and J_O–I curves and return key quantities defining the curves, and evaluated its performance against NH model and observations.

MATERIALS AND METHODS

Plant Material and Measurements of Leaf Gas Exchange and Chlorophyll Fluorescence

The experiment was conducted in the Yucheng Comprehensive Experiment Station of the Chinese Academy of Science. The detailed descriptions about soil and meteorological conditions in this experiment station were referred to Ye et al. (2019; 2020). Winter wheat was planted on October 4th, 2011 and the measurements were conducted on April 23th, 2012. Soybean was sown in on May 6th, 2013, and the measurements were performed on 27th July, 2013. Using the Li-6400-40 portable photosynthesis system (Li-Cor, Lincoln, NE, USA), measurements on leaf gas exchange and chlorophyll fluorescence were simultaneously performed on mature fully-expanded sun-exposed leaves in sunny days. J was calculated as $J = \Phi_{\text{PSII}} \times I \times 0.5 \times 0.84$, where Φ_{PSII} is the effective quantum yield of PSII (Genty et al., 1989; Krall and Edward, 1992).

For soybean, A_n–I curves and J–I curves were generated from applying different light intensities in a descending order of 2000, 1800, 1600, 1400, 1200, 1000, 800, 600, 400, 200, 150, 100, 80, 50, and 0 μmol m^{-2} s^{-1}. For winter wheat, the light intensity gradient started from 1800 μmol m^{-2} s^{-1} as the maximum, in alignment with environmental light availability from October to April. At each I step, CO_2 assimilation was monitored until a steady state was reached before logging a reading. Ambient CO_2 concentration in the cuvette (C_a) was kept constant at 380 μmol mol^{-1}. Leaf temperature in the cuvette was kept at about 30°C for winter wheat and 36°C for soybean, respectively. The observation-modeling intercomparison was conducted within each species.

A_n–I and J–I Analytical Models

NH model describes J–I curve as follows (Farquhar and Wong, 1984; von Caemmerer, 2000; von Caemmerer, 2013):

$$J = \frac{\alpha_e I + J_{\max} - \sqrt{(\alpha_e I + J_{\max})^2 - 4\alpha_e \theta J_{\max} I}}{2\theta} \quad (1)$$

where α_e is the initial slope of J–I curve, θ is the curve convexity, I is the light intensity, and $J_{\max}$ is the maximum electron transport rate.

NH model describes A_n–I curve as follows (Ögren and Evans, 1993; Thornley, 1998; von Caemmerer, 2000):

$$A_n = \frac{\alpha I + A_{\text{nmax}} - \sqrt{(\alpha I + A_{\text{nmax}})^2 - 4\alpha\theta A_{\text{nmax}} I}}{2\theta} - R_d \quad (2)$$

where α is the initial slope of A_n–I curve, A_{nmax} is the maximum net photosynthetic rate, and R_d is the dark respiration rate when

I = 0 μmol m^{-2} s^{-1}. NH model cannot return the corresponding saturation light intensities for J_{max} or A_{nmax} due to its asymptotic function.

The model developed by Ye et al. (2013, 2019; hereafter, Ye model) describes J–I curve as follows:

$$J = \alpha_e \frac{1-\beta_e I}{1+\gamma_e I} I \quad (3)$$

where α_e is the initial slope of J–I curve, and β_e and γ_e are the photoinhibition coefficient and light-saturation coefficient of J–I curve, respectively.

The saturation irradiance corresponding to the J_{max} ($I_{e\text{-}sat}$) can be calculated as follows:

$$I_{e-sat} = \frac{\sqrt{(\beta_e+\gamma_e)/\beta_e}-1}{\gamma_e} \quad (4)$$

Using Ye model, J_{max} can be calculated as follows:

$$J_{max} = \alpha_e \left(\frac{\sqrt{\beta_e+\gamma_e}-\sqrt{\beta_e}}{\gamma_e}\right)^2 \quad (5)$$

Ye model describes A_n–I curve as follows (Ye, 2007; Ye et al., 2013):

$$A_n = \alpha \frac{1-\beta I}{1+\gamma I} I - R_d \quad (6)$$

where α is the initial slope of A_n–I curve, β and γ are the photoinhibition coefficient and light-saturation coefficient of A_n–I curve, respectively.

The saturation irradiance corresponding to A_{nmax} (I_{sat}) can be calculated as follows:

$$I_{sat} = \frac{\sqrt{(\beta+\gamma)/\beta}-1}{\gamma} \quad (7)$$

Using Ye model, A_{nmax} can be calculated as follows:

$$A_{nmax} = \alpha \left(\frac{\sqrt{\beta+\gamma}-\sqrt{\beta}}{\gamma}\right) - R_d \quad (8)$$

J_C and J_O Estimation and J_C –I and J_O –I Analytical Models

Combining measurements of gas exchange and chlorophyll fluorescence was a reliable and easy-to-use technique widely used to determine J_O and J_C (e.g., Peterson, 1990; Comic and Briantais, 1991). In C_3 plants, carbon assimilation and photorespiration are two closely linked processes catalyzed by the key photosynthetic enzyme—RuBP carboxylase/oxygenase. Photorespiration is considered as an alternative sink for light-induced photosynthetic electron, and as a process helping consume extra photosynthetic electrons under high irradiance or other stressors limiting CO_2 availability at Rubisco (Stuhlfauth et al., 1990; Valentini et al., 1995; Long and Bernacchi, 2003). When the other alternative electron sinks are ignored or kept constant, the electron flow is mainly allocated for RuBP carboxylation and RuBP oxygenation (e.g. Farquhar et al., 1980; von Caemmerer, 2000; Farquhar et al., 2001; Long and Bernacchi, 2003; von Caemmerer et al., 2009; Bernacchi et al., 2013; von Caemmerer, 2013), and J_C and J_O can be respectively calculated as follows (Valentini et al., 1995):

$$J_C = \frac{1}{3}\left[J + 8\left(A_n + R_{day}\right)\right] \quad (9)$$

$$J_O = \frac{2}{3}\left[J - 4\left(A_n + R_{day}\right)\right] \quad (10)$$

where R_{day} is the day respiration rate, and following Fila et al. (2006), R_{day} = 0.5 R_d. In this study, J_C and J_O values calculated from Eqs. 9 and 10 were viewed as experimental observations—to be compared with modelled values derived from NH model and Ye model, respectively.

Using the same J–I modeling framework by Ye model, the light response of J_C (J_C–I) can be described as follows:

$$J_C = \alpha_C \frac{1-\beta_C I}{1+\gamma_C I} I \quad (11)$$

where α_C is the initial slope of J_C–I curve, and β_C and γ_C are two coefficient of J_C–I curve. The maximum J_C ($J_{C\text{-}max}$) and the saturation irradiance corresponding to the $J_{C\text{-}max}$ ($I_{C\text{-}sat}$) can be calculated as follows:

$$J_{C-max} = \alpha_C \left(\frac{\sqrt{\beta_C+\gamma_C}-\sqrt{\beta_C}}{\gamma_C}\right)^2 \quad (12)$$

$$I_{C-sat} = \frac{\sqrt{(\beta_C+\gamma_C)/\beta_C}-1}{\gamma_C} \quad (13)$$

Using the same J–I modeling framework by Ye model, the light response of J_O (J_O–I) can be described as follows:

$$J_O = \alpha_O \frac{1-\beta_O I}{1+\gamma_O I} I \quad (14)$$

where α_O is the initial slope of J_O–I curve, and β_O and γ_O are two coefficient of J_O–I curve. The maximum J_O ($J_{O\text{-}max}$) and the saturation irradiance corresponding to the $J_{O\text{-}max}$ ($I_{O\text{-}sat}$) can be calculated as follows:

$$J_{O-max} = \alpha_O \left(\frac{\sqrt{\beta_O+\gamma_O}-\sqrt{\beta_O}}{\gamma_O}\right)^2 \quad (15)$$

$$I_{O-sat} = \alpha_O \frac{\sqrt{\beta_O+\gamma_O/\beta_O}-1}{\gamma_O} \quad (16)$$

Meanwhile, NH model can describe the J_C–I and J_O–I curves as follows:

$$J_C = \frac{\alpha_C I + J_{C-max} - \sqrt{(\alpha_C I + J_{C-max})^2 - 4\alpha_C \theta J_{C-max} I}}{2\theta} \quad (17)$$

where α_C is the initial slope of J_C–I curve, θ is the curve convexity, and $J_{C\text{-}max}$ is the maximum J_C, and

$$J_O = \frac{\alpha_O I + J_{O-max} - \sqrt{(\alpha_O I + J_{O-max})^2 - 4\alpha_O \theta J_{O-max} I}}{2\theta} \quad (18)$$

where α_O is the initial slope of J_O–I curve, θ is the curve convexity, and $J_{O\text{-max}}$ is the maximum J_O. NH model—Eqs. 17 and 18—cannot return the corresponding saturation light intensities for $J_{C\text{-max}}$ or $J_{O\text{-max}}$ due to its asymptotic function.

Statistical Analysis

Statistical tests were performed using the statistical package SPSS 18.5 statistical software (SPSS, Chicago, IL). One-Way ANOVA was used to examine differences between parameter values estimated by NH model, Ye model and observed values of each parameter (A_{nmax}, I_{sat}, J_{max}, $I_{e\text{-sat}}$, $J_{C\text{-max}}$, $I_{C\text{-sat}}$, $J_{O\text{-max}}$, $I_{O\text{-sat}}$, etc.). Goodness of fit of the mathematical model to experimental observations was assessed using the coefficient of determination (R^2 = 1 – SSE/SST, where SSE is the error sum of squares, and SST is the total sum of squares).

RESULTS

Light Response of A_n and J

Soybean and winter wheat exhibited an immediate and rapid initial increase of A_n (α) and J (α_e) with the increasing I (**Figure 1**

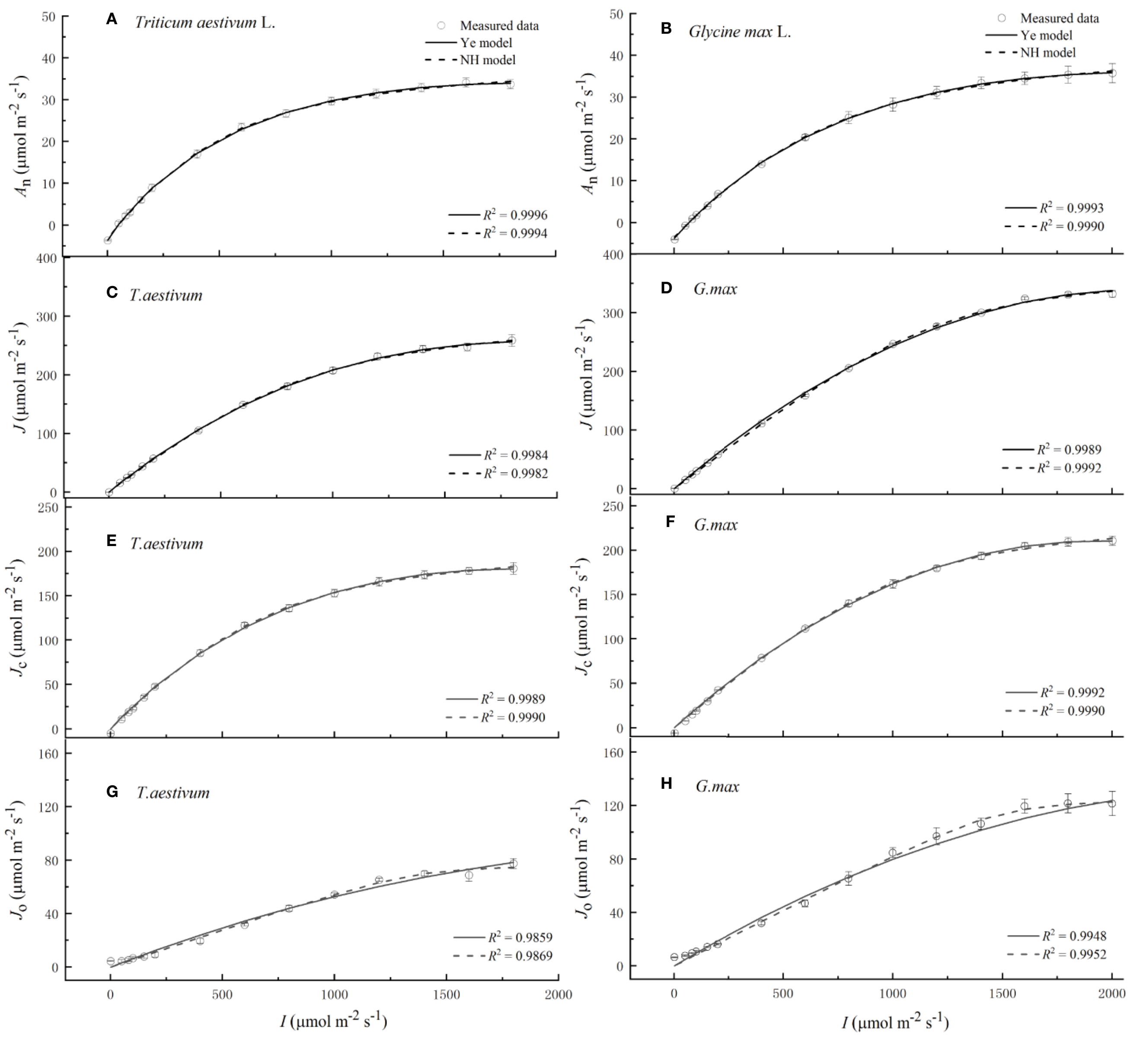

FIGURE 1 | Light response curves of net photosynthetic rate **(A, B),** electron transport rate **(C, D),** electron flow for RuBP carboxylation **(E, F)** and the electron flow for RuBP oxygenation **(G, H)** for winter wheat (*Triticum aestivum* L.) and soybean (*Glycine max* L.), respectively, over the irradiance range from 0 to 2000 µmol m^{-2} s^{-1}. Solid curves were fitted using Ye model, and dash curves were fitted using NH model. Values are means ± standard errors (n = 3).

and **Table 1**). The increase of A_n and J continued until I reached the cultivar-specific maximum values (A_{nmax} and J_{max}) at their corresponding saturation light intensities (I_{sat} and $I_{e\text{-}sat}$) (**Figure 1** and **Table 1**). Both NH model (Eqs. 1 and 2) and Ye model (Eqs. 3 and 6) showed high level of goodness of fit (R^2) to experimental observations of two species (**Figure 1** and **Table 1**). However, compared with observations, NH model significantly overestimated A_{nmax} and J_{max} ($P < 0.05$) for both soybean and winter wheat (**Table 1**). In contrast, A_{nmax} and J_{max} values returned by Ye model were in very close agreement with the observations for both species (**Table 1**).

Light Response of J_C and J_O

Both species exhibited an immediate and rapid initial increase of J_C (α_C) with the increasing I (**Figure 1** and **Table 1**). The increase of J_C continued until I reached the cultivar-specific maximum values ($J_{C\text{-max}}$) at the corresponding saturation light intensity ($I_{C\text{-sat}}$) (**Figure 1** and **Table 1**). Both Ye model (Eq. 11) and NH model (Eq. 17) showed high level of goodness of fit (R^2) to experimental observations of both species (**Figure 1** and **Table 1**). However, compared with observations, NH model significantly overestimated $J_{C\text{-max}}$ ($P < 0.05$) for both soybean and winter wheat (**Table 1**). In contrast, $J_{C\text{-max}}$ values returned by Ye model were in very close agreement with the observations for both species (**Table 1**).

Compared to the light-response rapidness of J_C, J_O exhibited a much slower initial increase (α_O) with the increasing I (**Figure 1** and **Table 1**). No species showed significant difference between the observed value of $J_{O\text{-max}}$ and that estimated by Ye model (Eq. 14) or NH model (Eq. 18) (**Table 1**). Both models showed high level of goodness of fit (R^2) to experimental observations of both species (**Figure 1** and **Table 1**).

TABLE 1 | Fitted (Ye model and NH model) and measured values (Obs.) of parameters defining the light-response curve of photosynthesis (A_n–I curve), electron transport rate (J–I curve), electron transport rate for RuBP carboxylation (J_C–I curve), and electron transport rate for RuBP oxygenation (J_O–I curve) for wheat and soybean species, respectively.

Parameters	*T. aestivum*			*G. max*		
	Ye model	NH model	Obs.	Ye model	NH model	Obs.
A_n–I curve						
θ (dimensionless)	–	0.659 ± 0.046	–	–	0.644 ± 0.073	–
α (μmol μmol $^{-1}$)	0.077 ± 0.005^a	0.069 ± 0.005^a	–	0.059 ± 0.002^a	0.055 ± 0.002^a	–
β (m^2 s μmol $^{-1}$)	(1.31 ± 0.07) × 10 $^{-4}$	–	–	(1.40 ± 0.08) × 10 $^{-4}$	–	–
γ (m^2 s μmol $^{-1}$)	(1.02 ± 0.16) × 10 $^{-3}$	–	–	(5.76 ± 0.43) × 10 $^{-4}$	–	–
A_{nmax} (μmol m^{-2} s^{-1})	33.91 ± 1.14^b	43.30 ± 1.28^a	33.71 ± 1.12^b	36.04 ± 2.11^b	47.74 ± 2.08^a	35.74 ± 2.29^b
I_{sat} (μmol m^{-2} s^{-1})	1870.58 ± 26.45^a	–	1799.59 ± 0.78^a	2199.05 ± 78.46^a	–	1999.73 ± 0.79^a
I_c (μmol m^{-2} s^{-1})	50.08 ± 6.61^a	50.42 ± 6.71 ^{a}	50.20 ± 6.67^a	66.72 ± 2.93^a	67.38 ± 2.81^a	66.82 ± 2.95^a
R_d (μmol m^{-2} s^{-1})	3.60 ± 0.21^a	3.29 ± 0.15^a	3.73 ± 0.14^a	3.76 ± 0.26^a	3.58 ± 0.13^a	4.03 ± 0.08^a
Residuals	1.12 ± 0.15^a	1.52 ± 0.34^a	–	2.26 ± 0.14^a	2.94 ± 0.84^a	–
J–I curve						
θ (dimensionless)	–	0.816 ± 0.009	–	–	0.924 ± 0.005	–
α_e (μmol μmol $^{-1}$)	0.295 ± 0.012^a	0.282 ± 0.012^a	–	0.299 ± 0.006^a	0.282 ± 0.005^a	–
β_e (m^2 s μmol $^{-1}$)	(2.42 ± 0.28) × 10 $^{-3}$	–	–	(3.07 ± 0.08) × 10 $^{-4}$	–	–
γ_e (m^2 s μmol $^{-1}$)	(1.26 ± 0.66) × 10 $^{-4}$	–	–	(-1.50 ± 0.24) × 10 $^{-4}$	–	–
J_{max} (μmol m^{-2} s^{-1})	257.23 ± 7.36^b	304.91 ± 7.11^a	261.56 ± 7.32^b	332.79 ± 5.16^b	373.87 ± 5.47^a	332.86 ± 5.01^b
$I_{e\text{-}sat}$ (μmol m^{-2} s^{-1})	1873.37 ± 109.46^a	–	1734.16 ± 66.15^a	1906.01 ± 19.97^a	–	1933.23 ± 66.27^a
Residuals	197.76 ± 119.18^a	224.69 ± 81.52^a	–	69.69 ± 6.00^a	139.25 ± 19.30^a	–
J_C–I curve						
θ (dimensionless)	–	0.770 ± 0.040	–	–	0.871 ± 0.011	–
α_C (μmol μmol $^{-1}$)	0.266 ± 0.012 a	0.248 ± 0.014^a	–	0.221 ± 0.003^a	0.207 ± 0.002^b	–
β_C (m^2 s μmol $^{-1}$)	(2.07 ± 0.10) × 10 $^{-4}$	–	–	(2.54 ± 0.03) × 10 $^{-4}$	–	–
γ_C (m^2 s μmol $^{-1}$)	(3.75 ± 0.75) × 10 $^{-4}$	–	–	(1.67 ± 1.37) × 10 $^{-5}$	–	–
$J_{C\text{-max}}$ (μmol m^{-2} s^{-1})	180.49 ± 5.16^b	210.90 ± 4.85^a	182.48 ± 5.10^b	210.66 ± 4.79^b	242.42 ± 3.43^a	210.76 ± 5.15^b
$I_{C\text{-sat}}$ (μmol m^{-2} s^{-1})	1813.42 ± 12.16^a	–	1734.16 ± 66.15^a	1938.65 ± 0.66^b	–	1999.73 ± 0.79^a
Residuals	72.25 ± 21.53^a	62.74 ± 8.96^a	–	78.54 ± 18.52^a	83.50 ± 5.26^a	–
J_O–I curve						
θ (dimensionless)	–	0.839 ± 0.159	–	–	0.987 ± 0.008	–
α_O (μmol μmol $^{-1}$)	0.062 ± 0.007^a	0.060 ± 0.007^a	–	0.087 ± 0.005^a	0.084 ± 0.005^a	–
β_O (m^2 s μmol $^{-1}$)	(3.45 ± 1.47) × 10 $^{-4}$	–	–	(4.12 ± 0.18) × 10 $^{-4}$	–	–
γ_O (m^2 s μmol $^{-1}$)	(-1.98 ± 2.75) × 10 $^{-4}$	–	–	(-3.71 ± 0.31) × 10 $^{-4}$	–	–
$J_{O\text{-max}}$ (μmol m^{-2} s^{-1})	85.67 ± 7.75^a	91.67 ± 16.52^a	79.08 ± 2.29^a	124.34 ± 7.51^a	127.13 ± 9.43^a	121.61 ± 9.14^a
$I_{O\text{-sat}}$ (μmol m^{-2} s^{-1})	2790.82 ± 1085.62^a	–	1734.16 ± 66.15^a	1860.92 ± 34.19^a	–	1866.73 ± 132.78^a
Residuals	145.10 ± 57.72^a	136.82 ± 60.25^a	–	147.28 ± 14.61^a	150.40 ± 13.62^a	–

For A_n–I curve, the parameters are: the initial slope of the A_n–I curve (α_p), the maximum A_n (A_{nmax}) and the corresponding saturation irradiance (I_{sat}), light compensation point (I_c) and dark respiration rate (R_d). For J–I curve, the parameters are: the initial slope of J–I curve (α_e), the maximum J (J_{max}) and the corresponding saturation irradiance corresponding to J_{max} ($I_{e\text{-}sat}$). For J_C–I curve, the parameters are: the initial slope of J_C–I curve (α_C), the maximum J_C ($J_{C\text{-max}}$) and the corresponding saturation irradiance corresponding to $J_{C\text{-max}}$ ($I_{C\text{-sat}}$). For J_O–I curve, the parameters are: the initial slope of J_O–I curve (α_O), the maximum J_O ($J_{O\text{-max}}$) and the corresponding saturation irradiance corresponding to $J_{O\text{-max}}$ ($I_{O\text{-sat}}$). The observation-modeling intercomparison was only conducted within each species. Within each species the different letters denote statistically significant differences between the values fitted by Ye model, NH model and measured values (Obs.) for each parameter ($P \leq 0.05$). Values are the mean ± standard errors (n = 3).

DISCUSSION

Assessed with an observation-modeling intercomparison approach, the results in this study highlight the robustness of Ye model in accurately reproducing A_n–I, J–I, J_C–I, and J_O–I curves and returning key quantities defining the curves, in particular: A_{nmax}, J_{max}, $J_{C\text{-}max}$, and $J_{O\text{-}max}$. On the contrary, the NH model significantly overestimates A_{nmax}, J_{max}, and $J_{C\text{-}max}$ (**Table 1**). For the first time, our study discloses the previously widely reported overestimation of J_{max} (and A_{nmax}) by the NH model is linked to its overestimation of $J_{C\text{-}max}$ but not $J_{O\text{-}max}$.

The overestimation of A_{nmax} by NH model found in this study is consistent with the previous reports (e.g., Calama et al., 2013; dos Santos et al., 2013; Lobo et al., 2014; Ježilová et al., 2015; Mayoral et al., 2015; Ogawa, 2015; Park et al., 2016; Quiroz et al., 2017; Poirier-Pocovi et al., 2018; Ye et al., 2020). The accurate returning of A_{nmax} by Ye model found in this study is consistent with previous studies using Ye model for various species under different environmental conditions (e.g., Wargent et al., 2011; Zu et al., 2011; Xu et al., 2012a; Xu et al., 2012b; Lobo et al., 2014; Xu et al., 2014; Song et al., 2015; Chen et al., 2016; Ye et al., 2019; Yang et al., 2020; Ye et al., 2020). The robustness of Ye model has also been validated for microalgae observations, including four freshwater and three marine microalgae species (Yang et al., 2020). The Ye model reproduced the A_n–I response well for all microalgae species, and produced I_{sat} closer to the measured values than those by three widely used models for microalgae (Yang et al., 2020). Meanwhile, the overestimation of J_{max} by NH model found in this study supports Buckley and Diaz-Espejo (2015) in highlighting the demerit of the asymptotic function (i.e. NH model).

One key novelty of the present study is its evaluation of both asymptotic and nonasymptotic functions in describing the light response of electron flow allocation for carboxylation and oxygenation respectively (i.e. J_C–I and J_O–I curves). To the best of our knowledge, this is the first study which has experimentally evidenced the robustness of a nonasymptotic function (Eqs. 3, 11, 14) in accurately (1) reproducing J–I, J_C–I, and J_O–I curves and (2) returning J_{max}, $J_{C\text{-}max}$, and $J_{O\text{-}max}$ values, as well as their corresponding the saturation light intensities. These novel findings are of significance for our understanding of light responses of plant carbon assimilation and photorespiration—both are catalyzed by RuBP carboxylase/oxygenase.

The findings, and the approach of bridging experiment and modeling, in the present study remain to be tested for (1) species of different plant function types and/or climatic origin, which could exhibit different response patterns (Ye et al., 2020) and (2) plant response to interaction of multiple environmental factors (e.g., temperature, rainfall pattern, soil type) involving fluctuating light. The explicit and consistent modeling framework and parameter definitions on light responses (i.e. A_n–I, J–I, J_C–I, and J_O–I)—combined with the simplicity and robustness—allows for future transparent scaling-up of leaf-level findings to whole-plant and ecosystem scales.

CONCLUSIONS

Ye model can accurately estimate A_{nmax}, J_{max}, and $J_{C\text{-}max}$ which the NH model would overestimate. Adopting an explicit and transparent analytical framework and consistent definitions on A_n–I, J–I, J_C–I, and J_O–I curves, this study highlights the advantage of Ye model over NH model in terms of (1) its extremely well reproduction of J–I, J_C–I, and J_O–I trends over a wide I range from light-limited to light-inhibitory light intensities, (2) accurately returning the wealth of key quantities defining J–I, J_C–I, and J_O–I curves, particularly J_{max}, $J_{C\text{-}max}$, $J_{O\text{-}max}$, and their corresponding the saturation light intensities (besides A_{nmax} and I_{sat} of A_n–I curve), and (3) being transparent in disclosing that the previously widely reported but poorly explained problem of NH model—overestimation of J_{max} (and the maximum plant carboxylation capacity)—is linked to its overestimation of $J_{C\text{-}max}$ but not $J_{O\text{-}max}$. Besides, NH model cannot obtain their saturation light intensities corresponding to J_{max}, A_{nmax}, $J_{C\text{-}max}$, and $J_{O\text{-}max}$ due to its asymptotic function. This study is of significance for both experimentalists and modelers working on better representation of photosynthetic processes under dynamic irradiance conditions.

DATA AVAILABILITY STATEMENT

The raw data supporting the conclusions of this article will be made available by the authors, without undue reservation.

AUTHOR CONTRIBUTIONS

All authors contributed to the conception of the work. H-JK mainly performed the experiment. Z-PY and S-XZ drafted the original manuscript. All authors critically reviewed and revised the manuscript with new data sets and contributed substantially to the completion of the present study. All authors contributed to the article and approved the submitted version.

FUNDING

This research was supported by the Natural Science Foundation of China (Grant No. 31960054 and 31560069) and the Key Science and Technology Innovation Team Project of Wenzhou City (Grant No. C20150008).

REFERENCES

Aspinwall, M. J., King, J. S., McKeand, S. E., and Domec, J. C. (2011). Leaf-level gas-exchange uniformity and photosynthetic capacity among loblolly pine (*Pinus taeda* L.) genotypes of contrasting inherent genetic variation. *Tree Physiol.* 31, 78–91. doi: 10.1093/treephys/tpq107

Bellasio, C., Beerling, D. J., and Griffiths, H. (2015). An Excel tool for deriving key photosynthetic parameters from combined gas exchange and chlorophyll fluorescence: Theory and practice. *Plant Cell Environ.* 39, 1180–1197. doi: 10.1111/pce.12560

Bernacchi, C. J., Bagley, J. E., Serbin, S. P., Ruiz-Vera, U. M., Rosenthal, D. M., and Vanloocke, A. (2013). Modelling C_3 photosynthesis from the chloroplast to the ecosystem. *Plant Cell Environ.* 36, 1641–1657. doi: 10.1111/pce.12118

Berry, J. A., and Farquhar, G. D. (1978). "The CO2 concentrating function of C4 photosynthesis: a biochemical model," in *The Proceedings of the Fourth International Congress on Photosynthesis*. Eds. D. Hall, J. Coombs and T. Goodwin (London: Biochemical Society of London), 119–131.

Buckley, T. N., and Diaz-Espejo, A. (2015). Reporting estimates of maximum potential electron transport rate. *New Phytol.* 205, 14–17. doi: 10.1111/nph.13018

Busch, F. A., and Sage, R. F. (2017). The sensitivity of photosynthesis to O_2 and CO_2 concentration identifies strong Rubisco control above the thermal optimum. *New Phytol.* 213, 1036–1051. doi: 10.1111/nph.14258

Cai, C., Li, G., Yang, H. L., Yang, J. H., Liu, H., Struik, P. C., et al. (2018). Do all leaf photosynthesis parameters of rice acclimate to elevated CO_2, elevated temperature, and their combination, in FACE environments? *Global Change Biol.* 24, 1685–1707. doi: 10.1111/gcb.13961

Calama, R., Puértolas, J., Madrigal, G., and Pardos, M. (2013). Modeling the environmental response of leaf net photosynthesis in *Pinus pinea* L. natural regeneration. *Ecol. Model.* 51, 9–21. doi: 10.1016/j.ecolmodel.2012.11.029

Chen, Z. Y., Peng, Z. S., Yang, J., Chen, W. Y., and Ou-Yang, Z. M. (2011). A mathematical model for describing light-response curves in nicotiana tabacum l. *Photosynthetica* 49, 467–471. doi: 10.1007/s11099-011-0056-5

Chen, X., Liu, W. Y., Song, L., Li, S., Wu, C. S., and Lu, H. Z. (2016). Adaptation of epiphytic bryophytes in the understorey attributing to the correlations and trade-offs between functional traits. *J. Bryol.* 38, 110–117. doi: 10.1080/03736687.2015.1120370

Comic, G., and Briantais, J. M. (1991). Partitioning of photosynthetic electron flow between CO_2 and O_2 reduction in a C_3 leaf (*Phaseolus vulgaris* L.) at different CO_2 concentrations and during drought stress. *Planta* 183, 178–184. doi: 10.1007/bf00197786

dos Santos, J. U. M., de Carvalho, G. J. F., and Fearnside, P. M. (2013). Measuring the impact of flooding on Amazonian trees: photosynthetic response models for ten species flooded by hydroelectric dams. *Trees* 27, 193–210. doi: 10.1007/s00468-012-0788-2

Farquahr, G. D., and Busch, F. A. (2017). Changes in the chloroplastic CO_2 concentration explain much of the observed Kok effect: a model. *New Phytol.* 214, 570–584. doi: 10.1111/nph.14512

Farquhar, G. D., and Wong, S. C. (1984). An empirical model of stomatal conductance. *Aus. J. Plant Physiol.* 11, 191–210. doi: 10.1071/pp9840191

Farquhar, G. D., von Caemmerer, S., and Berry, J. A. (1980). A biochemical model of photosynthetic CO_2 assimilation in leaves of C_3 species. *Planta* 149, 78–90. doi: 10.1007/BF00386231

Farquhar, G. D., von Caemmerer, S., and Berry, J. A. (2001). Models of photosynthesis. *Plant Physiol.* 125, 42–45. doi: 10.1104/pp.125.1.42

Fila, G., Badeck, F., Meyer, S., Cerovic, Z., and Ghashghaie, J. (2006). Relationships between leaf conductance to CO_2 diffusion and photosynthesis in micropropagated grapevine plants, before and after *ex vitro* acclimatization. *J. Exp. Bot.* 57, 2687–2695. doi: 10.1093/jxb/erl040

Genty, B., Briantais, J. M., and Baker, N. R. (1989). The relationship between the quantum yield of photosynthetic electron transport and quenching of chlorophyll fluorescence. *Biochim. Biophys. Acta* 990, 87–92. doi: 10.1016/s0304-4165(89)80016-9

Ježilová, E., Nožková-Hlaváčková, V., and Duchoslav, M. (2015). Photosynthetic characteristics of three ploidy levels of *Allium oleraceum* L. (Amaryllidaceae) differing in ecological amplitude. *Plant Spec. Biol.* 30, 212–224. doi: 10.1111/1442-1984.12053

Krall, J. P., and Edward, G. E. (1992). Relationship between photosystem II activity and CO_2 fixation in leaves. *Physiol. Plant* 86, 180–187. doi: 10.1111/j.1399-3054.1992.tb01328.x

Lobo, F. D. A., Barros, M. P. D., Dalmagro, H. J., Dalmolin, Â.C., Pereira, W. E., de Souza, É.C., et al. (2014). Fitting net photosynthetic light-response curves with microsoft excel – a critical look at the models. *Photosynthetica* 52, 445–456. doi: 10.1007/s11099-014-0045-6

Long, S. P., and Bernacchi, C. J. (2003). Gas exchange measurements, what can they tell us about the underlying limitations to photosynthesis? Procedures and sources of error. *J. Exp. Bot.* 54, 2393–2401. doi: 10.1093/jxb/erg262

Mayoral, C., Calama, R., Sánchez-González, M., and Pardos, M. (2015). Modelling the influence of light, water and temperature on photosynthesis in young trees of mixed Mediterranean forests. *New For.* 46, 485–506. doi: 10.1007/s11056-015-9471-y

Ogawa, K. (2015). Mathematical consideration of the pipe model theory in woody plant species. *Trees* 29, 695–704. doi: 10.1007/s00468-014-1147-2

Ögren, E., and Evans, J. R. (1993). Photosynthetic light-response curves. *Planta* 189, 182–190. doi: 10.1007/BF00195075

Park, K. S., Bekhzod, K., Kwon, J. K., and Son, J. E. (2016). Development of a coupled photosynthetic model of sweet basil hydroponically grown in plant factories. *Hortic. Environ. Biotechnol.* 57, 20–26. doi: 10.1007/s13580-016-0019-7

Peterson, R. B. (1990). Effects of irradiance on the *in vivo* CO_2:O_2 specificity factor in tobacco using simultaneous gas exchange and fluorescence techniques. *Plant Physiol.* 94, 892–898. doi: 10.1104/pp.94.3.892

Poirier-Pocovi, M., Lothier, J., and Buck-Sorlin, G. (2018). Modelling temporal variation of parameters used in two photosynthesis models: influence of fruit load and girdling on leaf photosynthesis in fruit-bearing branches of apple. *Ann. Bot.* 121, 821–832. doi: 10.1093/aob/mcx139

Quiroz, R., Loayza, H., Barreda, C., Gavilán, C., Posadas, A., and Ramírez, D. A. (2017). Linking process- based potato models with light reflectance data: Does model complexity enhance yield prediction accuracy? *Europ. J. Agron.* 82, 104–112. doi: 10.1016/j.eja.2016.10.008

Song, L., Zhang, Y. J., Chen, X., Li, S., Lu, H. Z., Wu, C. S., et al. (2015). Water relations and gas exchange of fan bryophytes and their adaptations to microhabitats in an Asian subtropical montane cloud forest. *J. Plant Res.* 128, 573–584. doi: 10.1007/s10265-015-0721-z

Stuhlfauth, T. R., Scheuermann, R., and Foek, H. P. (1990). Light energy dissipation under water stress conditions. Contribution of reassimilation and evidence for additional processes. *Plant Physiol.* 92, 1053–1061. doi: 10.1104/pp.92.4.1053

Sun, J. S., Sun, J. D., and Feng, Z. Z. (2015). Modelling photosynthesis in flag leaves of winter wheat (*Triticum aestivum*) considering the variation in photosynthesis parameters during development. *Funct. Plant Biol.* 42, 1036–1044. doi: 10.1071/FP15140

Thornley, J. H. M. (1998). Dynamic model of leaf photosynthesis with acclimation to light and nitrogen. *Ann. Bot.* 81, 431–430. doi: 10.1006/anbo.1997.0575

Valentini, R., Epron, D., Angelis, P. D., Matteucci, G., and Dreyer, E. (1995). *In situ* estimation of net CO_2 assimilation, photosynthetic electron flow and photorespiration of Turkey oak (*Q. cerris* L.) leaves: diurnal cycles under different water supply. *Plant Cell Environ.* 18, 631–640. doi: 10.1111/j.1365-3040.1995.tb00564.x

von Caemmerer, S., and Furbank, R. T. (1999). "Modeling of C4 photosynthesis," in *C4 Plant Biology*. Eds. R. F. Sage and R. Monson (San Diego, CA: Academic Press), 169–207.

von Caemmerer, S., Farquhar, G. D., and Berry, J. A. (2009). "Biochemical model of C3 photosynthesis," in *Photosynthesis in Silico. Understanding Complexity from Molecules to Ecosystemns*. Eds. A. Laisk, L. Nedbal and Govindjee, (Dordrecht, Netherlands: Springer), 209–230.

von Caemmerer, S. (2000). *Biochemical Models of Leaf Photosynthesis* (Victoria, Australia: Csiro Publishing).

von Caemmerer, S. (2013). Steady-state models of photosynthesis. *Plant Cell Environ.* 36, 1617–1630. doi: 10.1111/pce.12098

Walker, B. J., Orr, D. J., Carmo-Silva, E., Parry, M. A., Bernacchi, C. J., and Ort, D. R. (2017). Uncertainty in measurements of the photorespiratory CO_2 compensation point and its impact on models of leaf photosynthesis. *Photosyn. Res.* 132, 245–255. doi: 10.1007/s11120-017-0369-8

Wargent, J. J., Elfadly, E. M., Moore, J. P., and Paul, N. D. (2011). Increased exposure to uv-b radiation during early development leads to enhanced photoprotection and improved long-term performance in lactuca sativa. *Plant Cell Environ.* 34, 1401–1413. doi: 10.1111/j.1365-3040.2011.02342.x

Xu, Z. F., Yin, H. J., Xiong, P., Wan, C., and Liu, Q. (2012a). Short-term responses of *Picea asperata* seedlings of different ages grown in two contrasting forest ecosystems to experimental warming. *Environ. Exp. Bot.* 77, 1–11. doi: 10.1016/j.envexpbot.2011.10.011

Xu, Z. F., Hu, T. X., and Zhang, Y. B. (2012b). Effects of experimental warming on phenology, growth and gas exchange of treeline birch (*Betula utilis*) saplings, Eastern Tibetan Plateau, China. *Eur. J. For. Res.* 131, 811–819. doi: 10.1007/s10342-011-0554-9

Xu, J. Z., Yu, Y. M., Peng, S. Z., Yang, S. H., and Liao, L. X. (2014). A modified nonrectangular hyperbola equation for photosynthetic light-response curves of leaves with different nitrogen status. *Photosynthetica* 52, 117–123. doi: 10.1007/s11099-014-0011-3

Xu, J., Lv, Y., Liu, X., Wei, Q., and Liao, L. (2019). A general non-rectangular hyperbola equation for photosynthetic light response curve of rice at various leaf ages. *Sci. Rep.* 9, 9909. doi: 10.1038/s41598-019-46248-y

Yang, X. L., Liu, L. H., Yin, Z. K., Wang, X. Y., Wang, S. B., and Ye, Z. P. (2020). Quantifying photosynthetic performance of phytoplankton based on photosynthesis–irradiance response models. *Environ. Sci. Eur.* 32, 24. doi: 10.1186/s12302-020-00306-9

Yao, X., Zhou, H., Zhu, Q., Li, C. H., Zhang, H. J., Hu, J. J., et al. (2017). Photosynthetic response of soybean leaf to wide light-fluctuation in maize-soybean intercropping system. *Front. Plant Sci.* 8, 1695. doi: 10.3389/fpls.2017.01695

Ye, Z. P., Suggett, J. D., Robakowski, P., and Kang, H. J. (2013). A mechanistic model for the photosynthesis-light response based on the photosynthetic electron transport of PS II in C_3 and C_4 species. *New Phytol.* 152, 1251–1262. doi: 10.1111/nph.12242

Ye, Z. P., Liu, Y. G., Kang, H. J., Duan, H. L., Chen, X. M., and Zhou, S. X. (2019). Comparing two measures of leaf photorespiration rate across a wide range of light intensities. *J. Plant Physiol.* 240, 153002. doi: 10.1016/j.jplph.2019.153002

Ye, Z.-P., Ling, Y., Yu, Q., Duan, H.-L., Kang, H.-J., Huang, G.-M., et al. (2020). Quantifying light response of leaf-scale water-use efficiency and its interrelationships with photosynthesis and stomatal conductance in C_3 and C_4 Species. *Front. Plant Sci.* 11, 374. doi: 10.3389/fpls.2020.00374

Ye, Z. P. (2007). A new model for relationship between irradiance and the rate of photosynthesis in *Oryza sativa*. *Photosynthetica* 45, 637–640. doi: 10.1007/s11099-007-0110-5

Zu, Y. G., Wei, X. X., Yu, J. H., Li, D. W., Pang, H. H., and Tong, L. (2011). Responses in the physiology and biochemistry of Korean pine (*Pinus koraiensis*) under supplementary UV-B radiation. *Photosynthetica* 49, 448–458. doi: 10.1007/s11099-011-0057-4

Conflict of Interest: S-XZ was employed by the company The New Zealand Institute for Plant and Food Research Limited.

The remaining authors declare that the research was conducted in the absence of any commercial or financial relationships that could be construed as a potential conflict of interest.